Measurement 230 (2024) 114563

Contents lists available at ScienceDirect

Measurement

journal homepage: www.elsevier.com/locate/measurement

Optimizing pile bearing capacity prediction: Insights from dynamic testing and smart algorithms in geotechnical engineering

Hadi Fattahi [a], Hossein Ghaedi [a], Farshad Malekmahmoodi [a], Danial Jahed Armaghani [b,*]

[a] Faculty of Earth Sciences Engineering, Arak University of Technology, Arak, Iran
[b] School of Civil and Environmental Engineering, University of Technology Sydney, Sydney, NSW 2007, Australia

ARTICLE INFO

Keywords:
Pile bearing capacity
Fruit fly optimization algorithm
Invasive weed optimization algorithm
Sensitivity analysis
Dynamic tests

ABSTRACT

In contemporary mining and geotechnical projects, various approaches are employed to predict the bearing capacity of piles (Q_u). However, accurately modeling pile behavior using numerical, experimental, analytical, and regression methods proves challenging and, at times, infeasible due to the intricate nature of geotechnical materials, uncertainties, and the interaction between soil and piles. Consequently, formulations are generally presented, incorporating assumptions and simplifications that deviate from the actual complexity of the problem. Moreover, despite the high accuracy of pile loading tests as a reliable method in various design stages, their high costs and time requirements deter designers from conducting field tests. To address these challenges, this study performed 50 dynamic tests (HSDT) on precast concrete piles in Indonesia, Pekanbaru, to generate the necessary datasets. To mitigate experimental costs, two optimization algorithms fruit fly optimization (FFO) and invasive weed optimization (IWO) were employed. These models incorporated pile set (*S*), drop height (*H*), hammer weight (*W*), cross-sectional area (*A*), and length (*L*) as input parameters. Finally, the models' accuracy was evaluated using squared correlation coefficient (R^2), variance accounted for (VAF), mean square error (MSE), mean absolute percentage error (MAPE), and root mean square error (RMSE). The results revealed that the FFO algorithm achieved an accuracy range of 0.971–0.978. Similarly, the IWO algorithm exhibited an accuracy range of 0.984–0.988. Additionally, sensitivity analysis indicated that, among the input parameters, *W* had the most significant impact on the Q_u in both algorithms.

1. Introduction

In scenarios where the underlying soil beneath structures lacks the required strength to bear the loads of superstructures, pile foundations are utilized. These crucial substructure elements effectively transfer applied loads to deeper soil layers, and the resistances of both the pile toe and pile shaft play a pivotal role in forming the mechanism for weight transfer [1]. The interaction between the pile and the supporting soil introduces complexity to pile behavior under load. Calculating the weight-bearing capacity of piles (Q_u) involves various methods, primarily based on their geotechnical and geometrical characteristics. Determining the pile loading bearing capacity poses a significant geotechnical challenge, considering the intricate behavior of the soil and the interaction between the soil and the structure. Various scholars have proposed forecasting techniques, including numerical, regression, analytical, and experimental methods, to predict Q_u [2–4].

The accuracy of these anticipated values influences the reliability of the approaches, and each method can yield different results. Experimental and analytical techniques often lack precision due to non-uniform specifications, input parameters, and simplifications in relationships and assumptions. Similarly, numerical and regression methods face challenges in estimating the actual value of Q_u due to soil and pile parameter variability and the complexity of pile-soil interaction. In practice, the two primary methods for determining Q_u are the high strain dynamic load test (HSDT) and the pile static load test (SLT) [5]. The HSDT is preferred over SLT due to its quicker, more sophisticated, and cost-effective technology. While SLT is criticized for its time and cost intensity, HSDT employs a one-dimensional wave propagation analyzer (PDA) based on a pile driving model. Standardized American procedures have helped standardize the HSDT testing process, and literature surveys suggest good agreement between SLT and PDA test results for Q_u [6]. Although HSDT is faster and more cost-effective than SLT, the need for numerous tests in each project adds to expenses and time requirements. Consequently, reducing the number of necessary

* Corresponding author.
E-mail address: danial.jahedarmaghani@uts.edu.au (D.J. Armaghani).

https://doi.org/10.1016/j.measurement.2024.114563
Received 1 January 2024; Received in revised form 8 March 2024; Accepted 21 March 2024
Available online 22 March 2024

PDA tests can decrease the overall project cost. In pursuit of this goal, new technologies, such as soft computing, have emerged to forecast Q_u more accurately than current methods, requiring fewer tests and addressing engineering challenges more efficiently [7–11]. Hence, the adoption of AI-based and algorithmic approaches to tackle various geotechnical engineering issues, including the Q_u, has gained significant attention in recent years [12–33]. For instance, Luo et al. [34] introduced a hybrid intelligent model to evaluate the Q_u in sandy soils. They utilized a genetic algorithm-enhanced support vector machine (SVM) to develop their predictive model. Harandizadeh, Jahed Armaghani and Khari [35] employed the Adaptive Neural Fuzzy Inference System (ANFIS) to estimate Q_u by incorporating geometrical characteristics of soil and pile, SLT, and Cone Penetration Test (CPT) results. They enhanced their model's performance through the Particle Swarm Optimization (PSO) algorithm and the group way of data processing methodology. Chen et al. [36], referencing Momeni et al. [37] research, utilized Genetic Programming (GP) to determine the bearing capacity of deep foundations, asserting that the suggested neuro-imperialism prediction model proved to be a viable tool for forecasting Q_u. Shaik et al. [38] employed various soft computing techniques, considering input parameters such as pile length, pile size, soil internal friction angle, and vertical effective stress at the toe of the pile, recommending the use of an ANFIS model for Q_u anticipation. Samui [39] predicted Q_u using the support vector regression (SVR) method, concluding that SVR provides a close approximation to the real value with high accuracy. Acharyya and Dey [40] found Artificial Neural Networks (ANN) to be a practical approach for estimating strip footing load capacity near a sloping surface. They generated a substantial dataset using the finite element program PLAXIS, highlighting the friction angle among the model inputs as the most crucial factor. Nazir et al. [41] demonstrated the increased workability of ANN in predicting the stability of foundations with thin walls by incorporating the Imperialism Competitive Algorithm (ICA). Marto et al. [42] developed an ANN model based on PSO to assess the bearing capacity of shallow foundations, addressing ANN's susceptibility to local minima by using PSO. Their dataset included groundwater level, soil effective stress, soil friction angle, and findings from 40 published full-scale Standard Penetration Tests (SLTs) in granular materials as input factors. Pal [43] utilized the Generalized Regression Neural Network (GRNN) and pile drive recordings from 94 data series in soil to assess Q_u. The input parameters included pile elastic module, pile layout, driven hammer weight, pile height, pile surface, pile buried length, and hammer type. Alkroosh and Nikraz [44] employed the gene expression programming (GEP) model to establish an empirical equation for estimating the deep-seated axial ultimate bearing capacity in cohesive soils, particularly for pushed foundations. Maizir and Kassim [45] analyzed 300 datasets from global civil engineering projects in eastern Asia using ANNs to determine the axial capacity of driven piles. Kiefa [46] employed the GRNN approach to ascertain the axial capacity of driven piles in cohesionless soils, considering input parameters such as embedded length of the pile, overburden effective pressure, pile area, and angle of soil friction for modeling. Murlidhar et al. [47] employed two hybrid intelligent models, GA-ANN and PSO-ANN, to predict the Q_u. Their findings suggested that the PSO-ANN prediction model exhibited a closer match to the actual model, demonstrating higher efficiency compared to the GA-ANN model. Pham et al. [33] used ANN and Random Forest (RF) algorithms to predict the axial load capacity of piles, with results favoring the RF algorithm over ANN and other experimental methods. Sun et al. [48] investigated Q_u through a combined method of ANFIS and Firefly Algorithm (FA), resulting in a recommendation model with a high correlation coefficient ($R^2 = 0.997$). Alkroosh et al. [49] utilized Least Squares Support Vector Machine (LSSVM) algorithm results and CPT data for sandy and cone soils to predict piles' bearing capacities, demonstrating superior performance compared to traditional, experimental, and GEP methods. Zhang et al. [50] employed the ANFIS to estimate the final bearing capacity of precast reinforced concrete piles in Shanghai, China, using 42 data points. Nejad and Jaksa [51] constructed a multi-layer neural network (ANN-MLP) model based on CPT data to predict pile behavior, proving its superiority over traditional methods. Ahangar-Asr et al. [52] proposed an evolutionary polynomial regression (EPR) technique for predicting the lateral bearing capability of piles, demonstrating high accuracy compared to experimental methods. Benali and Nechnech [53] explored the viability of using ANN to forecast Q_u in sand, training the model with the geometric characteristics of 80 axially laden piles and relevant soil parameters. Pal and Deswal [54] utilized the SVM method to model the static Q_u with 105 dynamic wave-stress data, comparing the results with the generalized regression neural network method. Liu et al. [55] employed the SVM approach to create a model for determining the ultimate bearing capability of piles using data from 28 tests. Yong et al. [56] devised three soft computing methods— simulated annealing- genetic programming (GP) (SA-GP), GP tree-based, and ANFIS—to ascertain the Q_u. Muduli et al. [57] claimed that lateral pile load capacity could be estimated using an extreme learning machine. Fatehnia and Amirinia [58] reviewed the application of smart ANN-MLP and GP methods for estimating Q_u, asserting their suitability as alternatives to experimental and analytical methods. Jebur et al. [59] and Armaghani et al. [60] underscored the extensive utilization of artificial intelligence (AI) in deep foundations, expanding beyond the assessment of axial or lateral bearing capacity to encompass the measurement of pile settlement under compression loads.

According to the conducted research, since the bearing capacity of piles is very important in the construction and engineering structures, it is necessary to use methods that take into account the uncertainty in soil and rock parameters. One of the ways to consider the uncertainties in the values of the input parameters is to use field tests. Although this method has good accuracy for predicting the bearing capacity of piles, depending on the need in most large projects, a large number of these tests must be performed. In this case, due to the high repetition of field tests, it leads to an increase in costs and time. Also, in some cases, it will lead to fatigue of contractors and we will face human errors. According to the explanations provided, it is better to use indirect methods such as numerical, analytical, experimental and regression methods to predict the bearing capacity of piles. In numerical methods, because they accept only one value of the input parameters, we will have an output for each value of the input parameters. In this case, we will be faced with a large amount of output, which should be converted into a single model using statistical and probabilistic methods or intelligent methods to predict the bearing capacity of piles. In other words, numerical methods alone are not able to predict the bearing capacity of piles and these methods serve as probabilistic methods. Since all the projects related to the prediction of the bearing capacity of the piles are different from each other in all the case studies, it is not possible to use the experience of people in different projects. Also, in the analytical methods, due to the simplifications and assumptions that exist in the bearing capacity relationships of the piles, it is far from the reality of the problem and the accuracy of the model is greatly reduced. Also, regression methods are much less accurate compared to smart methods that improve the model at each iteration stage. For this reason, according to the explanations provided, many studies have been carried out using the above methods. But intelligent methods, taking into account the uncertainty in the input parameters, are able to perform analyzes and very complex (non-linear) models in a very short time with high accuracy, error and low cost. For this reason, in this paper to deal with this challenge, the current study proposes a robust method, which is an example of it by performing 50 PDA tests on precast concrete piles in Pekanbaru.

The study meticulously considers a set of five pivotal input parameters, recognizing their significant influence on the Q_u. In addressing the intrinsic nonlinearity and complexity of the model, the study employs two potent optimization algorithms: the Fruit Fly Optimization (FFO) and the Invasive Weed Optimization (IWO) Algorithms. Metaheuristic algorithms, exemplified by FFO and IWO, offer several advantages in prediction tasks. They excel in efficiently exploring complex solution

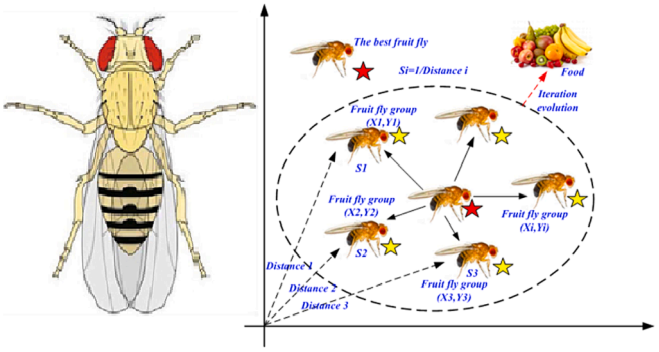

Fig. 1. Schematic representation of the algorithm for fruit flies.

spaces, navigating high-dimensional data, and delivering robust solutions. These algorithms provide global optimization capabilities, making them well-suited for tasks where finding the global optimum is crucial. Their adeptness in handling high-dimensional data, adaptability to various problem types, and inherent parallelizability contribute to their versatility, especially in large-scale prediction endeavors. Furthermore, their robustness in handling noisy and uncertain data, coupled with the maintenance of diverse solution populations, enhances their suitability for real-world prediction scenarios, promoting an effective exploration–exploitation balance. This inclusiveness transforms the models into valuable tools for estimating the Q_u with heightened accuracy. The approach outlined in this study not only addresses the limitations of traditional methods but also showcases a promising avenue for advancing the precision and reliability of bearing capacity predictions in geotechnical engineering.

2. Summary of utilized intelligent algorithms

2.1. Fruit fly optimization (FFO) algorithm

The FFO, originally proposed by Pan [61], stands as an innovative swarm intelligence technique inspired by the foraging behaviors of fruit flies. This algorithm falls within the realm of interactive evolutionary computation. Fruit flies, diminutive insects commonly found in temperate and tropical climates globally, serve as the biological inspiration for this method. Notably, fruit flies exhibit remarkable visual and olfactory capabilities in comparison to other species. Their sensory mechanisms enable them to swiftly detect various scents in the environment, with the remarkable ability to sense food sources up to 40 km away. Upon locating a food source, the fruit fly utilizes its keen sense of vision to navigate toward the target. The algorithm's procedural steps are established based on the foraging characteristics of these flies, as outlined in Fig. 1. This method draws parallels between the foraging patterns of fruit flies and the optimization process, creating an intelligent algorithm that leverages nature-inspired behaviors for solving complex computational problems.

Step 1: Randomly designate the initial location for the fruit fly swarm.

Step 2: Utilize Eq. (1) to assign a random distance and direction to each fruit fly, employing osphresis for the search of food.

$$X_i = X_{axis} + RandomValue \\ Y_i = Y_{axis} + RandomValue \tag{1}$$

Step 3: Conduct a search process based on smell, acknowledging that the precise position of the food source remains unknown. Determine the taste concentration judgment value (S), which is the reciprocal of the measured distance ($Dist$). Generate a population of fruit flies by randomly introducing several individuals in proximity to the existing fruit fly group.

$$Dist_i = \sqrt{X_i^2 + Y_i^2} \tag{2}$$

$$S_i = 1/Dist_i \tag{3}$$

Step 4: the judgment value representing the smell concentration (S) is incorporated into the judgment function for smell concentration. This process calculates the smell concentration ($Smell_i$) for the particular location of each fruit fly, which is also denoted as the fitness function.

$$Smell_i = function(S_i) \tag{4}$$

Step 5: Identify the fruit fly within the swarm possessing the highest scent concentration, effectively finding the maximum value.

$$[bestsmellbestindex] = \max(smell) \tag{5}$$

Step 6: Involves assessing and updating the information related to the best scent concentration detected by the fruit fly swarm. If the newly determined bestSmell value is found to be superior to the previously established bestSmell, the algorithm proceeds to update the Smellbest value and its corresponding location. This update is crucial for ensuring the fruit fly swarm's effective navigation towards the target location, utilizing its eyesight and maintaining the highest possible scent concentration value along with the associated position.

$$X\_axis = X(bestIndex) \quad Smellbest = bestsmell \quad Y\_axis = Y(bestIndex) \tag{6}$$

Step 7: the algorithm iterates through the process, including Steps 2 to 5, in a repetitive manner. During each iteration, the algorithm assesses whether the current scent concentration is better than that of the previous iteration. If the assessment is affirmative, the algorithm proceeds to Step 6 to update the best scent concentration value and its location. This iterative cycle continues until the algorithm determines that the current scent concentration meets the desired criteria or conditions. This dynamic process ensures the optimization of the swarm's navigation based on scent concentration in the pursuit of the target location.

2.2. Invasive weed optimization algorithm (IWO)

The IWO Algorithm, commonly referred to as IWO, was initially introduced by Mehrabian and Lucas [62]. The IWO algorithm belongs to the category of intelligent and evolutionary optimization algorithms, drawing inspiration from the reproductive, survival, and adaptive traits observed in weeds. This stochastic population-based metaheuristic optimization method emulates the colonization behavior of weeds in nature. Weeds, as a fundamental aspect of their activity, exhibit the growth of their population predominantly or exclusively in specific geographic regions, regardless of whether these regions are disproportionately extensive or limited. Weeds, as a natural phenomenon, exemplify a quest for optimality, actively seeking the ideal habitat for sustenance. They swiftly adapt to environmental changes and remain largely unaffected by them. Initially, weeds focus on prolific reproduction, increasing their quantity to cover the available environment (searching behavior). Subsequently, due to capacity constraints, they engage in competitive growth, enhancing the quality of their presence (greedy behavior).

The overall process of the IWO algorithm can be succinctly outlined as follows [62].

2.2.1. Reproduction

In the realm of reproduction, the algorithm permits each weed within the population to generate seeds in accordance with its unique fitness level and the collective fitness range of the entire colony. As a result, the number of seeds produced by an individual weed exhibits a linear increase, spanning from the minimum seed production associated

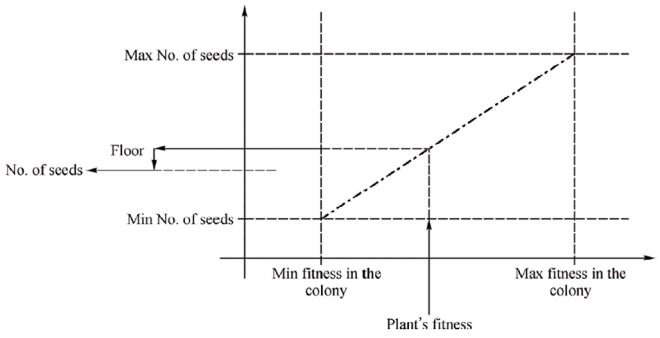

Fig. 2. A weed colony's process for producing seeds.

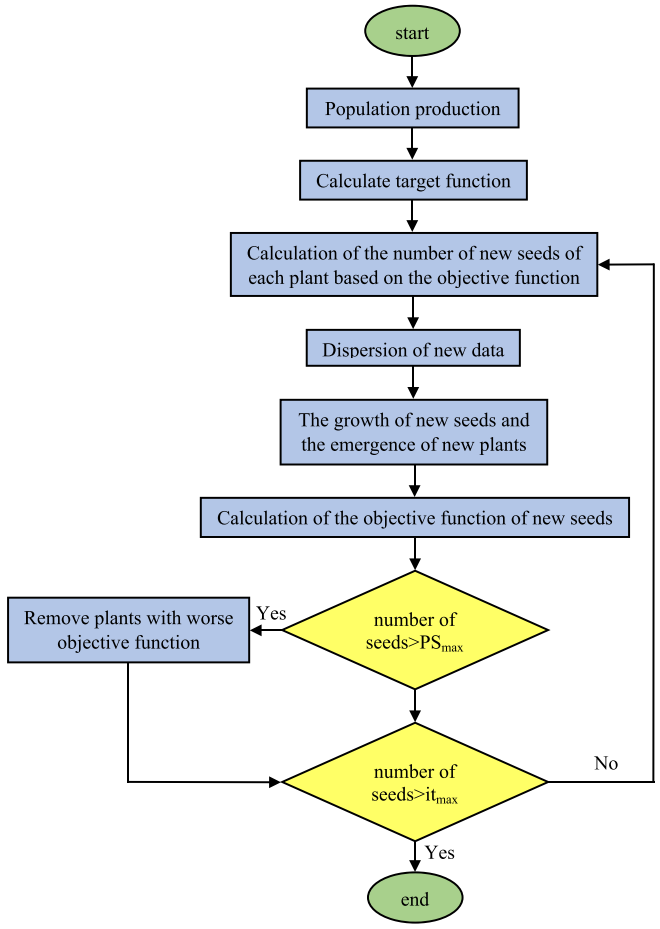

Fig. 3. Flow chart for IWO algorithm.

with a weed possessing the lowest fitness to the maximum seed production corresponding to a weed with the highest fitness. This mechanism ensures that the reproduction process aligns with the fitness characteristics of each weed, contributing to the overall genetic diversity and adaptive traits of the weed colony. Fig. 2 illustrates the linear correlation between the adaptation of each population member and seed production.

As depicted in Fig. 2, weeds exhibiting superior adaptation yield a greater number of seeds. The relationship governing seed production is expressed by Eq. (7) [62]:

$$Seed_n = \frac{f - f_{\min}}{f_{\max} - f_{\min}}(S_{\max} - S_{\min}) + S_{\min} \tag{7}$$

where $Seed_n$ represents the number of seeds produced, f denotes the compatibility of current weeds, f_{min} and f_{max} are the minimum and maximum compatibility within the current population, and S_{min} and S_{max} are the minimum and maximum possible seed production values, respectively.

2.2.2. Spatial dispersion

During this stage, random integers with a zero mean and variance σ^2 are appropriately distributed to randomly disperse the generated seeds across the D-dimensional search space. This ensures that the newly created seeds remain in close proximity to the parent seed, forming a local search area around each weed. The standard deviation (σ) of the random function gradually decreases from the initial defined value (σ_{final}) to the final value (σ_{final}), as expressed by Eq. (8).

$$\sigma_{iter} = \frac{(iter_{\max} - iter)^n}{(iter_{\max})^n}(\sigma_{initial} - \sigma_{final}) + \sigma_{final} \tag{8}$$

Here, σ_{iter} is the standard deviation value during the operational stage, $iter_{max}$ represents the maximum number of repetitions, and n is the nonlinearity index governing modulation or nonlinear oscillation. By implementing a nonlinear reduction in the likelihood of a seed landing in a distant location at each transformation stage, more compatible plants are clustered together, while incompatible ones are gradually eliminated.

2.2.3. Competitive elimination

When the number of weeds within the colony exceeds a specified maximum value, denoted as PSmaxPSmax, all newly generated seeds, along with their parent seeds, are collectively assessed in terms of the colony's fitness. To comply with the maximum permissible population size of the colony, weeds with lower fitness levels are systematically removed. This process offers an opportunity for weeds with lower fitness to reproduce, and if successful, they can endure in the lives of their offspring, provided they possess sufficient physical fitness. These steps are iteratively carried out until the seeds gradually converge toward the optimal outcome. The flowchart of the weed optimization algorithm is depicted in Fig. 3.

3. PDA test

The PDA test, also known as the HSDT ASTM D4945, serves as an indirect standard method for determining the Q_u. The test is grounded in the concept that any mechanical stress on uniformly shaped, small pile components, surrounded by more flexible materials, induces waves to propagate down the pile. For brevity, the partial differential equations governing wave propagation are not presented here. The PDA test involves evaluating force and velocity measurements recorded during the impact of a hammer on the pile to assess the distribution of soil resistance. When a pile is struck by a hammer, these characteristics are measured using strain gauges and accelerometers mounted on the pile's top. It is worth noting that the test may occasionally be referred to as a "re-strike test" due to its nature. Following a hammer strike, the force is calculated using wave analysis through a built-in application called CAPWAP in the pile drive analyzer. The calculated force is then compared to the force determined by strain gauges. CAPWAP employs iterative curve fitting to align the estimated and observed forces as closely as possible. During this iterative process, soil properties such as damping in CAPWAP are adjusted. Fig. 4 illustrates one of the PDA tests conducted at the location, showcasing sensors installed on the pile top for data collection. Since ASTM standardized the test, this section primarily aims to provide a concise overview of the test methodology, with additional information available in other studies [63–65].

4. Input and output data

In this study, a set of 50 restrike PDA tests conducted in a research

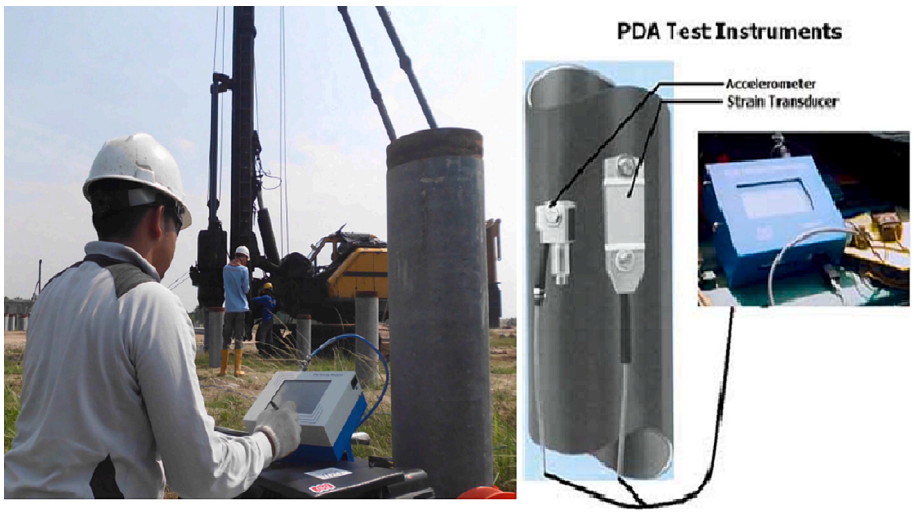

Fig. 4. PDA test for determining Q_u [37].

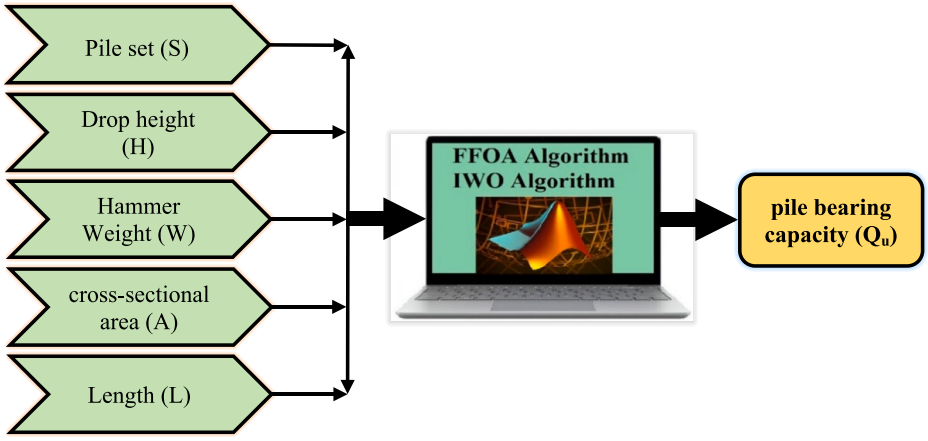

Fig. 5. Architecture of the FFO and IWO algorithms.

Table 1
Part of the input and output data values [37].

No	Inputs					Output
	S (mm)	H (m)	W (kN)	A (Cm^2)	L (m)	Q_U (kN)
1	3	1	20	282	8.6	1480
2	5	1	18	282	7.6	870
3	5	1	13	226	9.7	789
4	3	1	13	226	15.5	910
5	4	1	13	350	10.3	817
6	3	1	13	350	9.3	970
7	5	1	13	282	4.6	829
8	7	1	13	282	5.2	410
9	6	1	13	282	8.1	625
10	4	1	13	282	7.6	567
11	6	1	13	282	11.3	754
12	4	1	13	226	15	1102
13	5	1	13	226	11.2	950
14	0.1	1.5	53	400	33.6	2750
15	0.1	1.5	50	500	18.8	2522
16	0.1	1.5	50	500	18.6	2459
17	7	1	13	226	11	792
18	7	1	13	226	10.9	819
19	8	1	13	282	6.65	500
20	5	1	13	282	6.9	700

Table 2
Statistical analysis of the inputs and output data.

Statistical index	S (mm)	H (m)	W (kN)	A (cm^2)	L (m)	Q_u (kN)
Minimum	0.1	0.5	12	226	3.4	410
Maximum	8	4	63	500	33.6	3692
Mean	3.96	1.338	23.1	311.64	13.311	1284.1
Standard deviation	2.469	0.891	18	78.034	8.201	905.213

Table 3
Tuning parameters for the FFO.

Parameter	Value
Population Size	200
Maximum number of iterations	100

project by Momeni et al. [37] in Pekanbaru, Indonesia, on precast concrete piles was utilized to gather data for developing a predictive model for Q_u. The experiments employed equipment provided by Pile Dynamic, Inc., specifically a pile driving analyzer. The selection of appropriate input parameters is crucial for constructing a dataset for a predictive model. As illustrated in Fig. 5, the architectural model of the system involves five input parameters: pile set (*S*), drop height (*H*),

Table 4
Tuning parameters for the IWO.

Parameter	Value
Maximum number of iterations	3000
Initial Value of Standard Deviation	1
Maximum Number of Seeds	10
Maximum Population Size	100
Final Value of Standard Deviation	0.001
Initial Population Size	10
Minimum Number of Seeds	0

hammer weight (W), cross-sectional area (A), and length (L). Q_u is considered as the output parameter for model prediction. Table 1 presents the values of the five input parameters along with the corresponding Q_u determined by PDA.

In Table 2, comprehensive statistical analyses of both input and output datasets are presented, encompassing key parameters such as minimum values, maximum values, average values, and standard deviations. This tabulated information offers a detailed overview of the variability and distribution of the data, providing essential insights into the characteristics of the dataset under consideration.

5. Performance evaluation

To assess the effectiveness of the algorithms (FFO and IWO), various criteria have been employed for validation, including squared correlation coefficient (R^2), variance accounted for (VAF), mean square error (MSE), root mean square error (RMSE), and mean absolute percentage error (MAPE). Theoretically, optimal model performance is indicated when MAPE, RMSE, and MSE values approach zero, while R^2 and VAF values approach one. This signifies a high degree of accuracy in the generated model, suggesting minimal differences between projected and actual values, with errors approaching zero. The relationships governing VAF, R^2, MAPE, MSE, and RMSE indices are defined to quantify the accuracy and reliability of the models in predicting the desired outcomes [66–69].

$$VAF = \left[1 - \frac{var(Y_{mea} - Y_{pre})}{var(Y_{mea})}\right] \times 100 \tag{9}$$

$$R^2 = 1 - \frac{\sum_{k=1}^{n}(Y_{mea} - Y_{pre})^2}{\sum_{k=1}^{n} Y_{mea}^2 - \frac{\sum_{i=1}^{n} Y_{pre}^2}{n}} \tag{10}$$

$$MAPE = \frac{1}{n}\sum_{i=1}^{n}\left|Y_{mea} - Y_{pre}\right| \tag{11}$$

$$MSE = \frac{1}{n}\sum_{i=1}^{n}(Y_{mea} - Y_{pre})^2 \tag{12}$$

$$RMSE = \sqrt{\frac{1}{n}\sum_{i=1}^{n}(Y_{mea} - Y_{pre})^2} \tag{13}$$

In the provided equations, Y_{mea} represents the measured values of Q_u, Y_{pre} represents the predicted values, and n denotes the total number of samples in the dataset. These equations serve as a basis for comparing

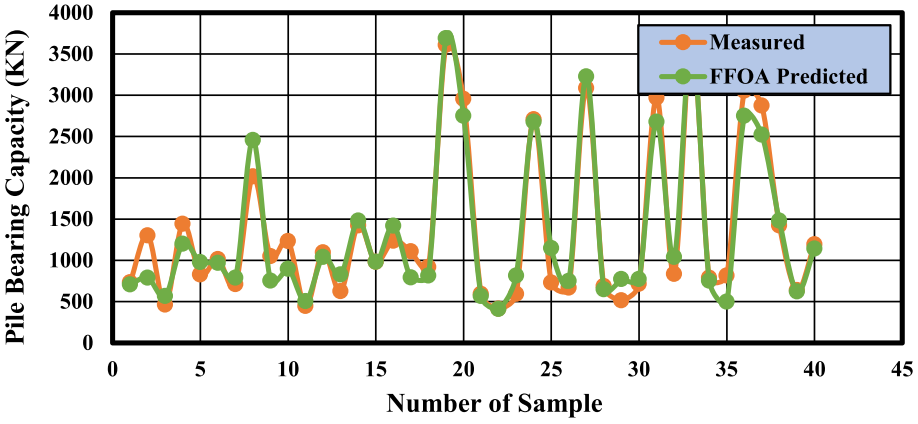

(a)

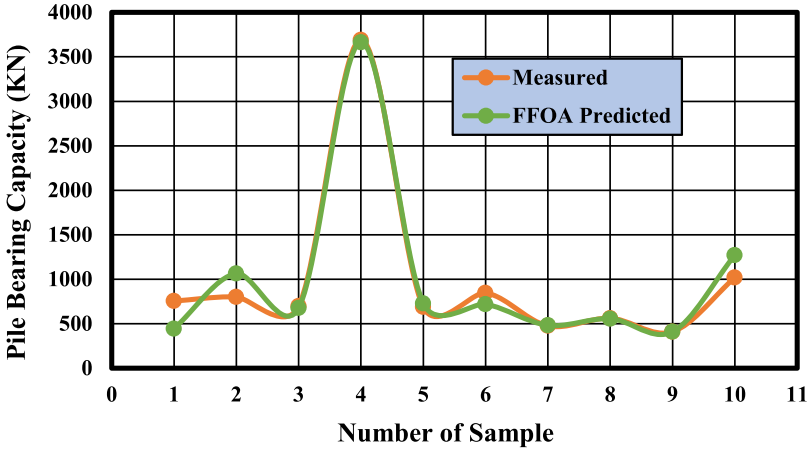

(b)

Fig. 6. Comparison Q_u predicted and measured by FFO algorithm for: (a) training, (b) testing.

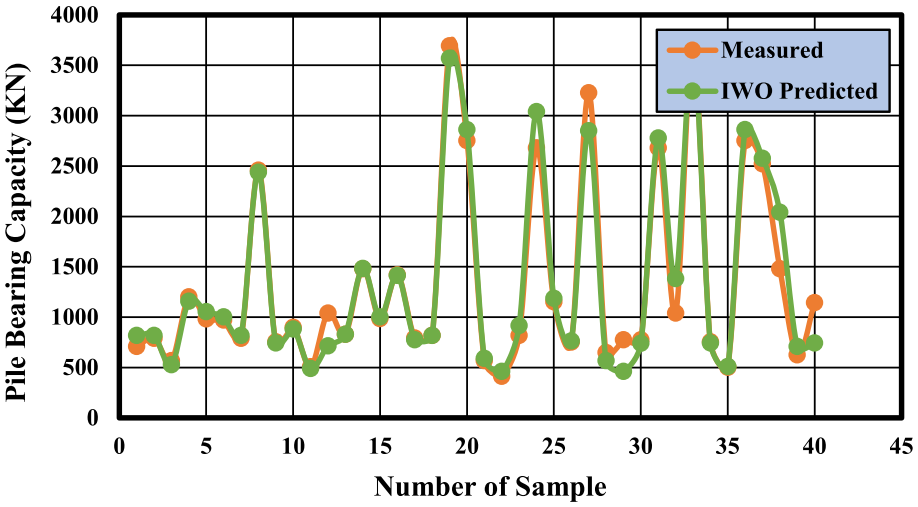

(a)

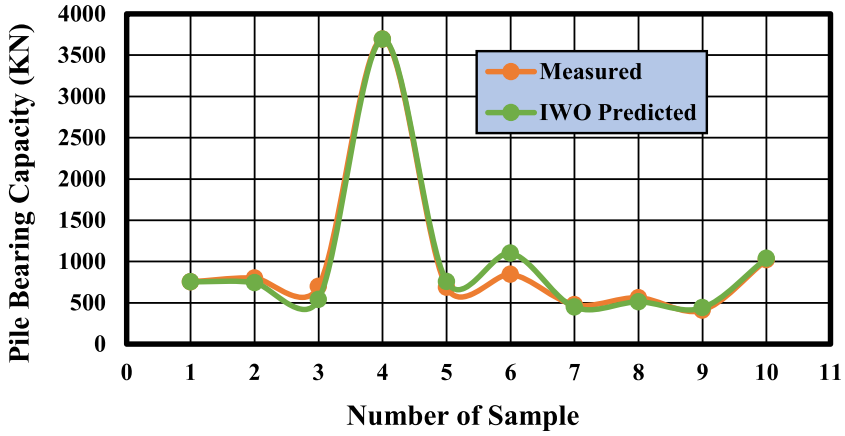

(b)

Fig. 7. Comparison of Q_u predicted and measured by IWO algorithm for: (a) training, (b) testing.

the actual measured values with the predicted values for evaluating the accuracy of the model [70–73].

6. Data preprocessing

Before conducting any calculations, data-driven system modeling techniques often undergo various preprocessing stages to eliminate outliers, incorrect data, or missing values. This ensures the appropriateness of the raw database used for modeling. All data samples are normalized to the range [0, 1] through the linear mapping function outlined below, facilitating training and enhancing prediction accuracy.

$$X_n = [(X_{mea} - X_{\min})/(X_{\max} - X_{\min})] \tag{14}$$

The normalization is denoted by X_n, representing the normalized value, X_{mea} for the real value, and X_{max} and X_{min} as the maximum and minimum values, respectively.

7. Discussion and model results

A dataset of 50 data points was used in this modeling effort, as detailed in the database section. For the purposes of modeling using PDA test results, the test results along with the inputs should be randomly divided into two subsets: one for training and the other for testing. In this article, 80 % of the data (40 data points) are dedicated to model construction, while the remaining 20 % (10 data points) are saved for model evaluation and validation. Subsequently, to predict the Q_u using FFO and IWO algorithms, a nonlinear equation (Eq. (15)) was derived using MATLAB coding:

$$Q_u = ((w_1 W) - (-w_2 H^2) \times (w_3 A^{w_4}) - (-w_5 L^2) - (-w_6 S)) - w_7 \tag{15}$$

The weighting factors for the input parameters are represented by the variable w_i in this equation, and the ideal values for those parameters are calculated via MATLAB optimization techniques. The following is the procedure that is used to determine the coefficients for the nonlinear equations that estimate Q_u for the FFO and IWO algorithms:

$$Q_u = ((0.4818W) - (-0.4239H^2) \times (0.758A^{0.9366}) - (-0.2083L^2) - (-0.2483S)) - 3.9803 \tag{16}$$

$$Q_u = ((0.3911W) - (-0.4071H^2) \times (0.801A^{0.89616}) - (-0.1083L^2) - (-0.1998S)) - 3.1082 \tag{17}$$

In every model that is coded in the MATLAB environment, the data must be called and the training of models and algorithms must begin. Most of the artificial intelligence models themselves have *meta*-parameters that must be adjusted by trial and error or in combination with optimization algorithms and placed in their best state and value every time the models are repeated and executed. In this case, the trained models also produce

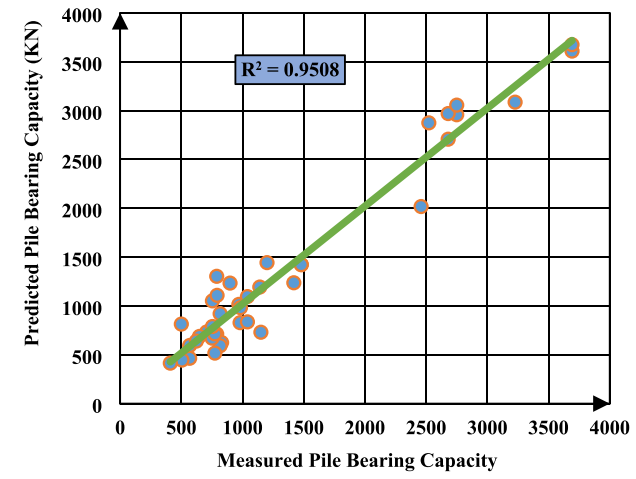

(a)

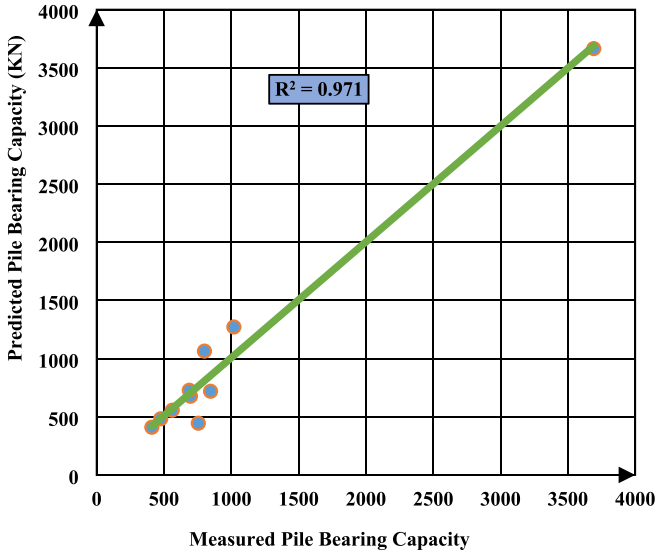

(b)

Fig. 8. Correlation between measured values of Q_u and values estimated by the FFO algorithm for: (a) training, (b) testing.

the best output with high accuracy and low error. For this reason, in order to predict the bearing capacity of the piles, in addition to the coding done for the FFOA and IWO algorithms the setting parameters of each algorithm should be created so that the cost function of the model reaches its lowest level. In this case, the created error will be closer to zero and the accuracy of the model will be higher. If the parameters of the algorithms are not set correctly, it can lead to wrong or misleading results. Therefore, it is critical to apply a successful optimization process to determine the appropriate values for these parameters. The values of FFO and IWO adjustment parameters are presented in Tables 3 and 4, respectively, according to the above description.

After modeling and fine-tuning influential parameters in the algorithms, a comparative analysis of the estimated Q_u values generated by the FFO and IWO algorithms was conducted against the measured values from the datasets during the training and testing stages. The results, as depicted in Figs. 6 and 7, demonstrate a high level of compatibility between the estimated and measured values.

Additionally, Figs. 8 and 9 depict the correlation between measured values obtained from datasets in both the testing and training phases and the predicted values of Q_u generated by the FFO and IWO algorithms.

To validate and ensure the accuracy of the relationships created by the FFO and IWO algorithms, a set of statistical parameters, as shown in Table 5, were employed for both training and testing data. The close-to-zero error and close-to-one accuracy values indicate high precision in the created model. The performance indices presented in Table 5 affirm that the use of FFO and IWO algorithms for model development performs well, making them reliable for estimating the Q_u.

According to the results obtained from the analysis, if the cost function of the obtained model tends to zero, the accuracy of the model will be higher and the error will be closer to zero. Fig. 10 shows the convergence of the model for 3000 iterations. As it is clear from the curve, the cost function of the model obtained by the algorithms approaches zero and has an acceptable performance.

8. Sensitivity analysis

The significance of parameters influencing Q_u, including W (kN), S (mm), L (m), H (m), and A (cm^2), is crucial in understanding the model's output. Employing sensitivity analysis, it becomes possible to discern which of these parameters has the most substantial impact on the Q_u. Utilizing @RISK software for this analysis enables the determination of correlation strength and ranking parameters. A value closer to 1 signifies a more positive correlation, while closeness to −1 indicates a more negative correlation, implying that changes in those parameters would have the greatest impact on Q_u. Rank values were computed by sorting data from least to greatest, and these values were assigned based on their position in the hierarchy. Figs. 11 and 12 illustrate the outcomes of sensitivity analysis corresponding to the models created by the FFO and IWO Algorithms, respectively. The sensitivity analysis results unequivocally reveal that parameter W exhibits the most significant influence on Q_u compared to the other model inputs.

9. Conclusions

In conclusion, assessing Q_u through the HSDT proves to be a time and cost-effective alternative to the SLT. However, the uncertainty inherent in soil and pile parameters necessitates repeated HSDT tests at various points, incurring additional costs and time. To address this challenge, researchers increasingly turn to soft computing methods for predicting Q_u. The results obtained from the article are summarized as follows:

- This study aims to forecast the Q_u using the FFO and IWO Algorithms. The research conducted 50 PDA tests in Pekanbaru, Indonesia, focusing on prestressed concrete piles with input parameters, including *S, H, A, W,* and *L*. During the model development stage, 80 % of the dataset, comprising 40 datasets, was randomly allocated for training purposes, with the remaining 20 % (10 datasets) earmarked for testing and validation.
- The effectiveness of the models was assessed through the utilization of five standard statistical indices: VAF, R^2, MAPE, MSE, and RMSE. The results demonstrated high accuracy, with VAF values of 94.605 (training) and 97.868 (testing), R^2 values of 0.95 (training) and 0.971 (testing), MAPE values of 160.801 (training) and 105.292 (testing), MSE values of 44578.5 (training) and 24857.8 (testing), and RMSE values of 211.136 (training) and 157.663 (testing). Furthermore, the FFO and IWO algorithms exhibited excellent predictive capabilities, with VAF values of 96.397 (training) and 98.402 (testing), R^2 values of 0.966 (training) and 0.988 (testing), MAPE values of 102.591 (training) and 66.859 (testing), MSE values of 29332.4 (training) and 10255.7 (testing), and RMSE values of 171.267 (training) and 101.271 (testing).
- The comparison between estimated and measured Q_u indicated close agreement, validating the reliability of the proposed models. Additionally, @RISK software was employed for sensitivity analysis, revealing that the parameter W has the most significant impact on Q_u in soils compared to other input parameters.

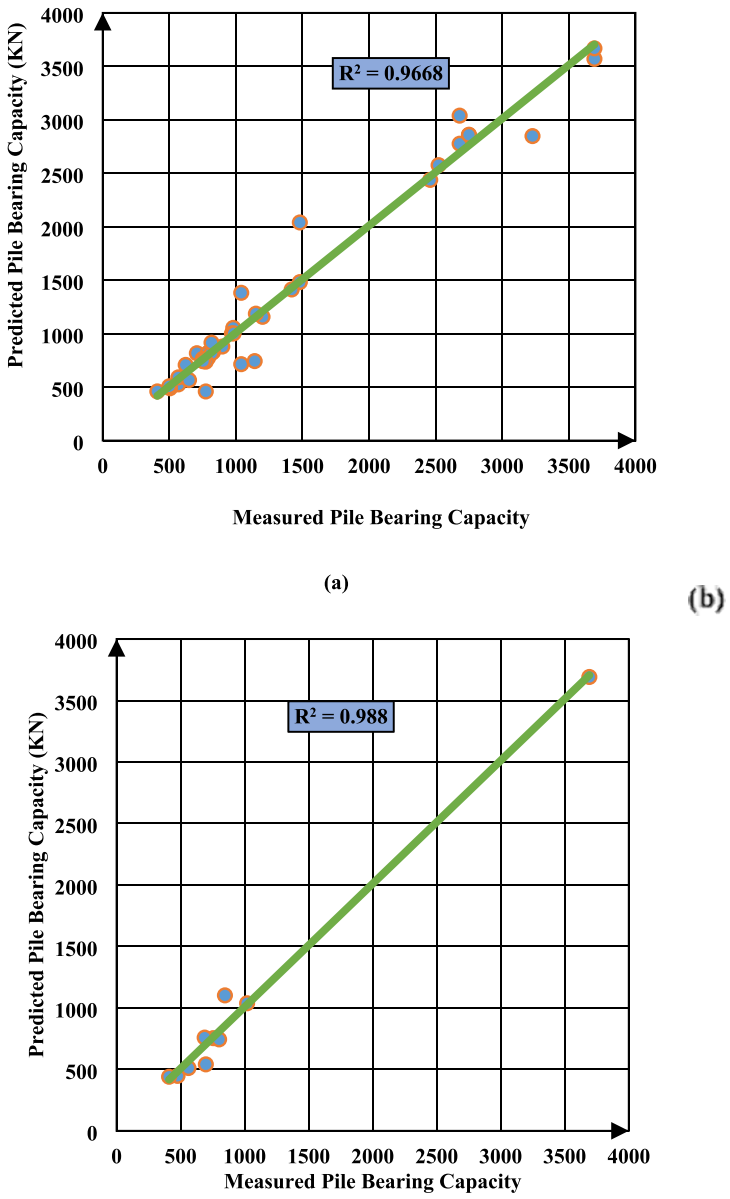

Fig. 9. Correlation between measured values of Q_u and values estimated by the IWO algorithm for: (a) training, (b) testing.

Table 5
The validation outcomes for the predictive connections employing FFO and IWO.

Algorithm type	Description	VAF (%)	R^2	MAPE	RMSE	MSE
FFO	Train	94.605	0.95082	160.801	211.136	44578.5
	Test	97.868	0.97138	105.292	157.663	24857.8
IWO	Train	96.397	0.96684	102.591	171.267	29332.4
	Test	98.402	0.98822	66.859	101.271	10255.7

- The established relationship in this study holds potential applicability across various study areas.

10. Compliance with ethical standards

Informed consent. Informed consent was obtained from all individual participants included in the study.

Data availability statement. All data and models generated or used during the study appear in the published study, and the code generated or used during the study is available from the corresponding author by request.

Ethical approval This study does not contain any studies with human participants or animals performed by any of the authors.

CRediT authorship contribution statement

Hadi Fattahi: Writing – review & editing, Writing – original draft, Supervision, Methodology, Data curation, Conceptualization. **Hossein Ghaedi:** Writing – review & editing, Writing – original draft, Methodology, Formal analysis. **Farshad Malekmahmoodi:** Writing – review & editing, Writing – original draft, Methodology, Formal analysis. **Danial Jahed Armaghani:** Writing – review & editing, Writing – original draft,

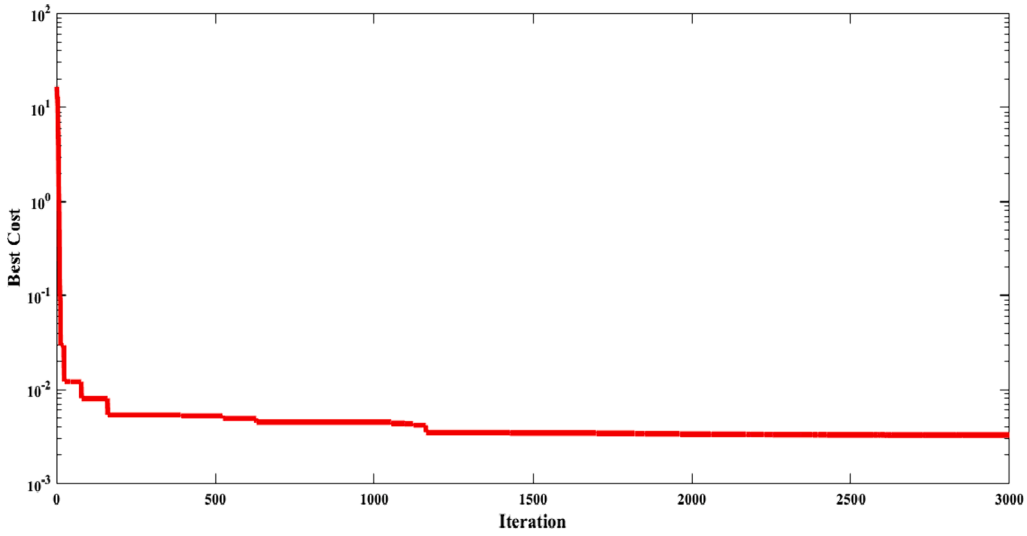

Fig. 10. Model convergence curve.

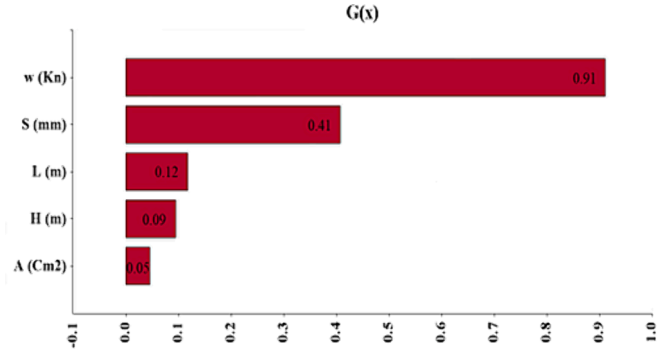

Fig. 11. The outcomes of sensitivity analysis for the relationship established by the FFO algorithm.

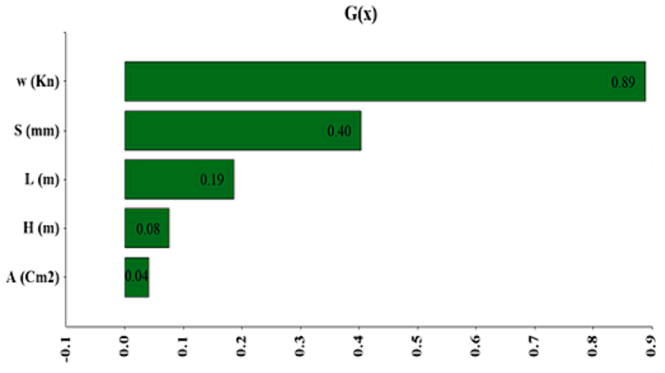

Fig. 12. The outcomes of sensitivity analysis for the relationship established by the IWO algorithm.

Supervision, Conceptualization.

Declaration of competing interest

The authors declare that they have no known competing financial interests or personal relationships that could have appeared to influence the work reported in this paper.

Data availability

Data will be made available on request.

References

[1] E. Momeni, R. Nazir, D.J. Armaghani, H. Maizir, Application of artificial neural network for predicting shaft and tip resistances of concrete piles, Earth Sci. Res. J. 19 (2015) 85–93.
[2] G.G. Meyerhof, Bearing capacity and settlement of pile foundations, J. Geotech. Eng. Div. 102 (1976) 197–228.
[3] H. Maizir, R. Suryanita, H. Jingga, Estimation of pile bearing capacity of single driven pile in sandy soil using finite element and artificial neural network methods, Int. J. Appl. Phys. Sci. 2 (2016).
[4] D. Jahed Armaghani, R.S.N.S.B.R. Shoib, K. Faizi, A.S.A. Rashid, Developing a hybrid PSO–ANN model for estimating the ultimate bearing capacity of rock-socketed piles, Neural Comput. Appl. 28 (2017) 391–405.
[5] A. Kordjazi, F.P. Nejad, M. Jaksa, Prediction of ultimate axial load-carrying capacity of piles using a support vector machine based on CPT data, Comput Geotech 55 (2014) 91–102.
[6] C. Chen, L. Shi, M. Shariati, A. Toghroli, E.T. Mohamad, D.T. Bui, M. Khorami, Behavior of steel storage pallet racking connection-a review, 2019.
[7] M.A. Shahin, M.B. Jaksa, H.R. Maier, Artificial neural network applications in geotechnical engineering, Aust. Geomech. 36 (2001) 49–62.
[8] M. Roosta, M. Ghaedi, A. Daneshfar, R. Sahraei, A. Asghari, Optimization of the ultrasonic assisted removal of methylene blue by gold nanoparticles loaded on activated carbon using experimental design methodology, Ultrason. Sonochem. 21 (2014) 242–252.
[9] M. Ghaedi, A. Ansari, M. Habibi, A. Asghari, Removal of malachite green from aqueous solution by zinc oxide nanoparticle loaded on activated carbon: kinetics and isotherm study, J. Ind. Eng. Chem. 20 (2014) 17–28.
[10] M. Roosta, M. Ghaedi, F. Yousefi, Optimization of the combined ultrasonic assisted/adsorption method for the removal of malachite green by zinc sulfide nanoparticles loaded on activated carbon: experimental design, RSC Adv. 5 (2015) 100129–100141.
[11] M.A. Shahin, A review of artificial intelligence applications in shallow foundations, Int. J. Geotech. Eng. 9 (2015) 49–60.
[12] D.J. Armaghani, M. Hasanipanah, H.B. Amnieh, E.T. Mohamad, Feasibility of ICA in approximating ground vibration resulting from mine blasting, Neural Comput. Appl. 29 (2018) 457–465.
[13] D.J. Armaghani, E.T. Mohamad, M.S. Narayanasamy, N. Narita, S. Yagiz, Development of hybrid intelligent models for predicting TBM penetration rate in hard rock condition, Tunn. Undergr. Sp. Tech. 63 (2017) 29–43.
[14] D.J. Armaghani, E. Tonnizam Mohamad, E. Momeni, M. Monjezi, M. Sundaram Narayanasamy, Prediction of the strength and elasticity modulus of granite through an expert artificial neural network, Arab. J. Geosci. 9 (2016) 1–16.
[15] E. Momeni, D.J. Armaghani, M. Hajihassani, M.F.M. Amin, Prediction of uniaxial compressive strength of rock samples using hybrid particle swarm optimization-based artificial neural networks, Measurement 60 (2015) 50–63.
[16] S. Hoseinie, M. Ataei, R. Mikaeil, Effects of microfabric on drillability of rocks, Bull. Eng. Geol. Envir 78 (2019) 1443–1449.
[17] F. Meng, X. Chen, Interval-valued intuitionistic fuzzy multi-criteria group decision making based on cross entropy and 2-additive measures, Soft. Comput. 19 (2015) 2071–2082.

[18] H. Yang, Z. Li, T. Jie, Z. Zhang, Effects of joints on the cutting behavior of disc cutter running on the jointed rock mass, Tunn. Undergr. Sp. Tech. 81 (2018) 112–120.
[19] P. Samui, D. Kim, Least square support vector machine and multivariate adaptive regression spline for modeling lateral load capacity of piles, Neural Comput. Appl. 23 (2013) 1123–1127.
[20] P. Samui, B. Dixon, Application of support vector machine and relevance vector machine to determine evaporative losses in reservoirs, Hydrol. Process. 26 (2012) 1361–1369.
[21] P. Samui, Support vector machine applied to settlement of shallow foundations on cohesionless soils, Comput. Geotech. 35 (2008) 419–427.
[22] R. Li, S. Hu, Y. Wang, M. Yin, A local search algorithm with tabu strategy and perturbation mechanism for generalized vertex cover problem, Neural Comput. Appl. 28 (2017) 1775–1785.
[23] R. Shirani Faradonbeh, D. Jahed Armaghani, M. Abd Majid, M. Md Tahir, B. Ramesh Murlidhar, M. Monjezi, H. Wong, Prediction of ground vibration due to quarry blasting based on gene expression programming: a new model for peak particle velocity prediction, Int. J. Environ. Sci. Technol. 13 (2016) 1453–1464.
[24] S. Shams, M. Monjezi, V.J. Majd, D.J. Armaghani, Application of fuzzy inference system for prediction of rock fragmentation induced by blasting, Arab. J. Geosci. 8 (2015) 10819–10832.
[25] Z. Jian, X.-Z. Shi, R.-D. Huang, X.-Y. Qiu, C. Chong, Feasibility of stochastic gradient boosting approach for predicting rockburst damage in burst-prone mines, Trans. Nonfer. Metal. Soc. China 26 (2016) 1938–1945.
[26] J. Zhou, X. Li, H.S. Mitri, Classification of rockburst in underground projects: comparison of ten supervised learning methods, J. Comput. Civil Eng. 30 (2016) 04016003.
[27] A. Toghroli, M. Mohammadhassani, M. Suhatril, M. Shariati, Z. Ibrahim, Prediction of shear capacity of channel shear connectors using the ANFIS model, Steel Compos. Struct. 17 (2014) 623–639.
[28] M. Shariat, M. Shariati, A. Madadi, K. Wakil, Computational Lagrangian Multiplier Method by using for optimization and sensitivity analysis of rectangular reinforced concrete beams, Steel Compos. Struct 29 (2018) 243–256.
[29] M. Safa, M. Shariati, Z. Ibrahim, A. Toghroli, S.B. Baharom, N.M. Nor, D. Petković, Potential of adaptive neuro fuzzy inference system for evaluating the factors affecting steel-concrete composite beam's shear strength, Steel Compos. Struct. An. Int. J. 21 (2016) 679–688.
[30] M. Wang, X. Shi, J. Zhou, Optimal charge scheme calculation for multiring blasting using modified harries mathematical model, J. Perform. Constr. Facil 33 (2019) 04019002.
[31] M.A. Benbouras, A.-I. Petrişor, H. Zedira, L. Ghelani, L. Lefilef, Forecasting the bearing capacity of the driven piles using advanced machine-learning techniques, Appl. Sci. 11 (2021) 10908.
[32] T. Bong, S.-R. Kim, B.-I. Kim, Prediction of ultimate bearing capacity of aggregate pier reinforced clay using multiple regression analysis and deep learning, Appl. Sci. 10 (2020) 4580.
[33] T.A. Pham, H.-B. Ly, V.Q. Tran, L.V. Giap, H.-L.-T. Vu, H.-A.-T. Duong, Prediction of pile axial bearing capacity using artificial neural network and random forest, Appl. Sci. 10 (2020) 1871.
[34] Z. Luo, M. Hasanipanah, H. Bakhshandeh Amnieh, K. Brindhadevi, M. Tahir, GA-SVR: a novel hybrid data-driven model to simulate vertical load capacity of driven piles, Eng Comput 37 (2021) 823–831.
[35] H. Harandizadeh, D. Jahed Armaghani, M. Khari, A new development of ANFIS–GMDH optimized by PSO to predict pile bearing capacity based on experimental datasets, Eng. Comput. 37 (2021) 685–700.
[36] W. Chen, P. Sarir, X.-N. Bui, H. Nguyen, M. Tahir, D., Jahed Armaghani, Neuro-genetic, neuro-imperialism and genetic programing models in predicting ultimate bearing capacity of pile, Eng. Comput. 36 (2020) 1101–1115.
[37] E. Momeni, R. Nazir, D.J. Armaghani, H. Maizir, Prediction of pile bearing capacity using a hybrid genetic algorithm-based ANN, Measurement 57 (2014) 122–131.
[38] S. Shaik, K. Krishna, M. Abbas, M. Ahmed, D. Mavaluru, Applying several soft computing techniques for prediction of bearing capacity of driven piles, Eng. Comput. 35 (2019) 1463–1474.
[39] P. Samui, Prediction of pile bearing capacity using support vector machine, Int. J. Geotech. Eng. 5 (2011) 95–102.
[40] R. Acharyya, A. Dey, Assessment of bearing capacity for strip footing located near sloping surface considering ANN model, Neural Comput. Appl. 31 (2019) 8087–8100.
[41] R. Nazir, E. Momeni, K. Marsono, Prediction of bearing capacity for thin-wall spread foundations using ICA-ANN predictive model, in: Proc. Int. Conf. Civil, Struct. Transp. Eng. Ottawa, Ontario, 2015.
[42] A. Marto, M. Hajihassani, E. Momeni, Bearing Capacity of Shallow Foundation's Prediction through Hybrid Artificial Neural Networks, Applied mechanics and materials, Trans Tech Publ, 2014, pp. 681-686.
[43] M. Pal, Modelling pile capacity using generalised regression neural network, in: Proceedings of Indian Geotechnical Conference December, 2011, pp. 15-17.
[44] I. Alkroosh, H. Nikraz, Predicting axial capacity of driven piles in cohesive soils using intelligent computing, Eng. Appl. Artif. Intel. 25 (2012) 618–627.
[45] H. Maizir, K.A. Kassim, Neural network application in prediction of axial bearing capacity of driven piles. Proceedings of the International Multiconference of Engineers and Computer Scientists, 2013.
[46] M.A. Kiefa, General regression neural networks for driven piles in cohesionless soils, J. Geotech. Geoenviron. 124 (1998) 1177–1185.
[47] B.R. Murlidhar, R.K. Sinha, E.T. Mohamad, R. Sonkar, M. Khorami, The effects of particle swarm optimisation and genetic algorithm on ANN results in predicting pile bearing capacity, Int. J. Hydromech. 3 (2020) 69–87.
[48] G. Sun, M. Hasanipanah, H.B. Amnieh, L.K. Foong, Feasibility of indirect measurement of bearing capacity of driven piles based on a computational intelligence technique, Measurement 156 (2020) 107577.
[49] I.S. Alkroosh, M. Bahadori, H. Nikraz, A. Bahadori, Regressive approach for predicting bearing capacity of bored piles from cone penetration test data, J. Rock Mech. Geotech. Eng. 7 (2015) 584–592.
[50] Z. Zhang, D. Ding, L. Rao, Z. Bi, An ANFIS based approach for predicting the ultimate bearing capacity of single piles, Foundation Analysis and Design: Innovative Methods, 2006, pp. 159–166.
[51] F.P. Nejad, M.B. Jaksa, Load-settlement behavior modeling of single piles using artificial neural networks and CPT data, Comput. Geotech. 89 (2017) 9–21.
[52] A. Ahangar-Asr, A.A. Javadi, A. Johari, Y. Chen, Lateral load bearing capacity modelling of piles in cohesive soils in undrained conditions: an intelligent evolutionary approach, Appl. Soft Comput. 24 (2014) 822–828.
[53] A. Benali, A. Nechnech, Prediction of the pile capacity in purely coherent soils using the approach of the artificial neural networks,, in: International Seminar Innovation and Valorization in Civil Engineering and Construction Materials, Morocco–rabat/november, 2011, pp. 23–25.
[54] M. Pal, S. Deswal, Modeling pile capacity using support vector machines and generalized regression neural network, J. Geotech. Geoenviron. Eng. 134 (2008) 1021–1024.
[55] Y.J. Liu, S.H. Liang, J.W. Wu, N. Fu, Prediction method of vertical ultimate bearing capacity of single pile based on support vector machine, in: Advanced Materials Research, Trans Tech Publ, 2011, pp. 2278–2282.
[56] W. Yong, J. Zhou, D. Jahed Armaghani, M. Tahir, R. Tarinejad, B.T. Pham, V. Van Huynh, A new hybrid simulated annealing-based genetic programming technique to predict the ultimate bearing capacity of piles, Eng Comput 37 (2021) 2111–2127.
[57] P.K. Muduli, S.K. Das, M.R. Das, Prediction of lateral load capacity of piles using extreme learning machine, Int. J. Geotech. Eng. 7 (2013) 388–394.
[58] M. Fatehnia, G. Amirinia, A review of genetic programming and artificial neural network applications in pile foundations, Int. J. Geo-Eng. 9 (2018) 1–20.
[59] A.A. Jebur, W. Atherton, R.M. Al Khaddar, E. Loffill, Artificial neural network (ANN) approach for modelling of pile settlement of open-ended steel piles subjected to compression load, Europ. J. Environ. Civil Eng. 25 (2021) 429–451.
[60] D.J. Armaghani, R.S. Faradonbeh, H. Rezaei, A.S.A. Rashid, H.B. Amnieh, Settlement prediction of the rock-socketed piles through a new technique based on gene expression programming, Neural Comput. Appl. 29 (2018) 1115–1125.
[61] W.-T. Pan, A new fruit fly optimization algorithm: taking the financial distress model as an example, Knowl.-Based Syst. 26 (2012) 69–74.
[62] A.R. Mehrabian, C. Lucas, A novel numerical optimization algorithm inspired from weed colonization, Eco. Inform. 1 (2006) 355–366.
[63] F. Rausche, G.G. Goble, G.E. Likins Jr, Dynamic determination of pile capacity, J. Geotech. Eng. 111 (1985) 367–383.
[64] G.G. Goble, F. Moses, F. Rausche, DYNAMIC STUDIES ON THE BEARING CAPACITY OF PILES PROJECT REPORT OF PHASE III, 1970.
[65] B.H. Fellenius, Wave equation analysis and dynamic monitoring, Deep Found J. 1 (1984) 49–55.
[66] H. Fattahi, A New method for forecasting uniaxial compressive strength of weak rocks, J. Min. Environ. 11 (2020) 505–515.
[67] H. Fattahi, N. Babanouri, RES-based model in evaluation of surface settlement caused by EPB shield tunneling, Indi Geotech. J. 48 (2018) 746–752.
[68] H. Fattahi, A. Moradi, Risk assessment and estimation of TBM penetration rate using RES-based model, Geotech. Geol. Eng. 35 (2017) 365–376.
[69] H. Fattahi, A. Moradi, A new approach for estimation of the rock mass deformation modulus: a rock engineering systems-based model, Bull. Eng. Geol. Envir. 77 (2018) 363–374.
[70] H. Fattahi, Application of improved support vector regression model for prediction of deformation modulus of a rock mass, Eng. Comput. 32 (2016) 567–580.
[71] H. Fattahi, Applying soft computing methods to predict the uniaxial compressive strength of rocks from schmidt hammer rebound values, Comput. Geosci. 21 (2017) 665–681.
[72] H. Fattahi, Risk assessment and prediction of safety factor for circular failure slope using rock engineering systems, Environ. Earth Sci. 76 (2017) 224.
[73] H. Fattahi, Applying rock engineering systems to evaluate shaft resistance of a pile embedded in rock, Geotech. Geol. Eng. 36 (2018) 3269–3279.